

Interval Q estimation and a quality indicator -- QQI

Chuandong (Richard) Xu and Robert R. Stewart

ABSTRACT

We use the spectral ratio method with zero-offset VSP data to develop a new approach to calculate the continuous interval Q_P value in Ross Lake area. A Q estimation Quality Indicator (QQI) for getting a stable Q has been established. This QQI curve also explains why sometimes we cannot get good results. Due to the much narrower frequency bandwidth of S-wave, Q_S estimation is not as good as Q_P .

INTRODUCTION

The spectral ratio method is widely used to determine an attenuation or Q factor from VSP data (Tonn, 1991). For any given two downhole geophones at depths d_1 and d_2 :

$$\frac{|A(\omega)_{d2}|}{|A(\omega)_{d1}|} = e^{-\frac{|\omega|}{2Q} \left(\frac{d_2}{v_2} - \frac{d_1}{v_1} \right)} \quad (1)$$

where $A(\omega)$ is the amplitude spectrum at depth d , $\omega=2\pi f$ is the frequency, v_1 and v_2 are the average velocities from surface to depth d_1 and d_2 , respectively. Expressed in time, equation (1) becomes:

$$\frac{|A(\omega)_{d2}|}{|A(\omega)_{d1}|} = e^{-\frac{|\omega|}{2Q} (t_2 - t_1)} \quad (2)$$

where t_1 and t_2 are travel time from source to geophones at depth d_1 and d_2 .

The standard way to calculate Q by equation (2) is to choose relatively widely spaced geophones from different depth ranges, i.e. shallow, middle and deep. Calculating their spectra ratios gives a relatively stable Q for a big chunk of depth interval. Averaging the amplitude spectra from a few adjacent geophones first is also commonly used. However, if using adjacent geophones to calculate their spectral ratio, the Q result often jumps back and forth, or is negative, which is physically impossible. Therefore, choosing which two geophones becomes a procedure of trial and error.

Some questions are arising: What controls the Q calculation? Can we obtain a continuous Q estimation? Under what conditions is a reasonable Q not possible?

In the following, we'll investigate the above questions.

The VSP data used in this paper are from Husky Energy Inc.'s Ross Lake oilfield, which is located in south-western Saskatchewan. There were two types of source for the zero-offset VSP: a vertical mini-vibrator with 12 s, 8-180 Hz sweep and a horizontal vibrator with 12 s 5-100 Hz sweep. For ease in discussing the zero-offset cases, we use "P-source" to represent the vertical-vibrator and "S-source" for the horizontal-vibrator.

There are 130 geophone levels ranging from depths of 198m to 1165m. The VSP survey well has a normal sonic log and a low quality V_S log.

The fact that both P and S-sources are available gives us an excellent example to study the attenuation of P- and S-waves, to estimate Q_P and Q_S using the same method, and to compare them. This work leads to a future study concerning the attenuation of PS-waves.

DATA PREPARATION

The best data for Q calculation are the zero-offset, downgoing wavefield traces: P- and S-waves propagate into the earth one-way and are recorded by downhole geophones.

First, the first-break times for the P-wave are picked on the P-source vertical-component data. A 5-by-5 alpha-trimmed weighted median filter is used to separate the downgoing wavefield from the total wavefield.

For the S-source horizontal-component data processing, the first step is to rotate the x- and y-component to radial- and transverse-component, which align energy in the source-receiver plane. A hodogram analysis is used for this horizontal two-component rotation using a 200ms time window following the arrival time roughly picked on x-component. The rotation result is showing in Figure 1.

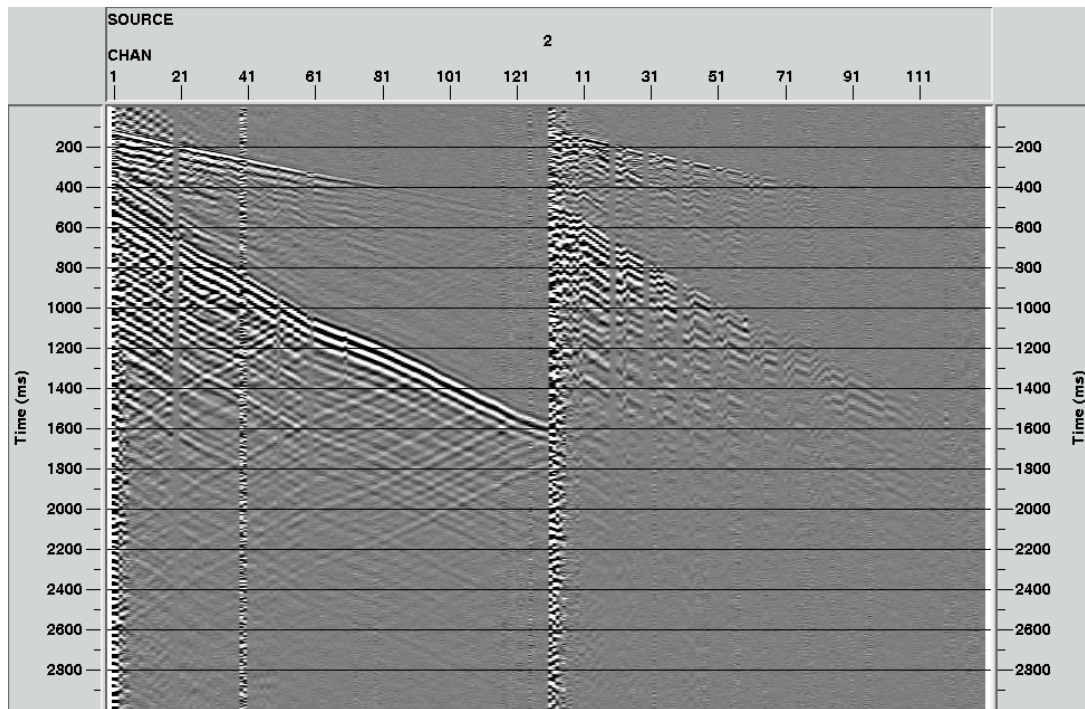


FIG. 1. The S-source horizontal component VSP data after rotation. The radial (left) and transverse (right) components are shown with one display scalar.

After rotation, the first arrival time is re-picked on the radial-component trace. Figure 2 shows the first breaks on downgoing P- and S-wave traces. The S-source radial component data are then flattened at the first break time, and applied the same median filter as for P-source data to extract the downgoing shear wavefield (Figure 3).

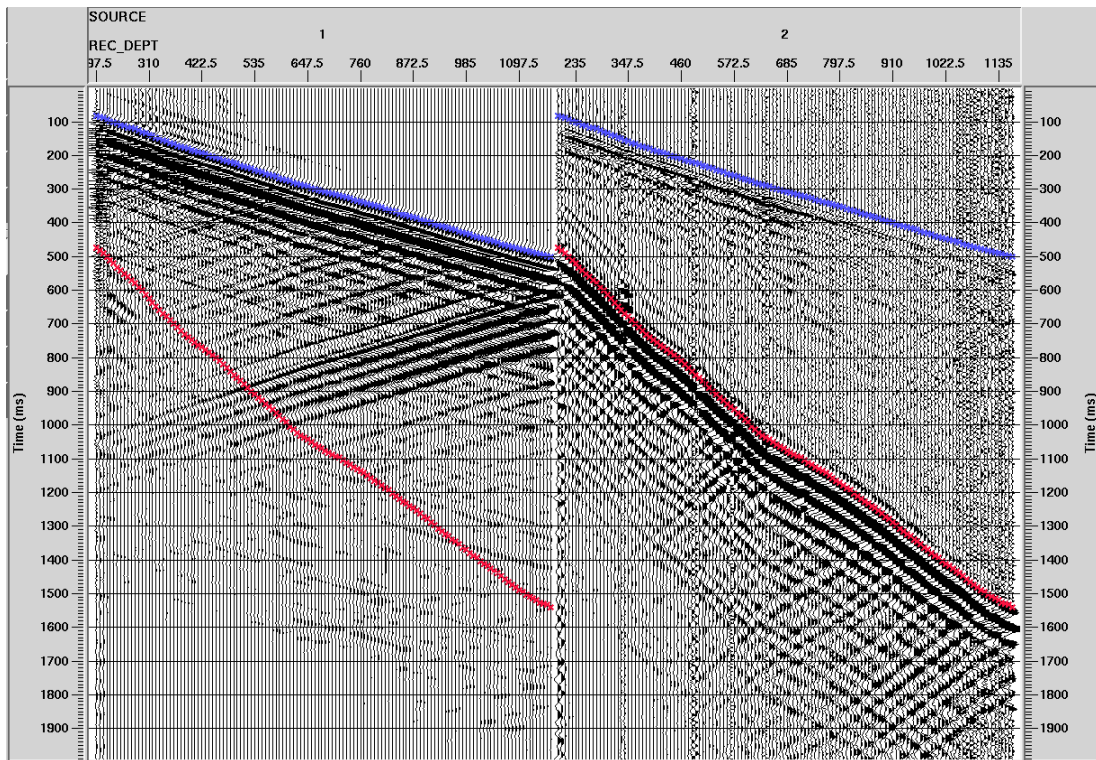


FIG. 2. P-wave first breaks (blue) and S-wave first breaks (red) are over imposed on P-source vertical (left) and S-source radial (right) components traces. AGC is applied for display.

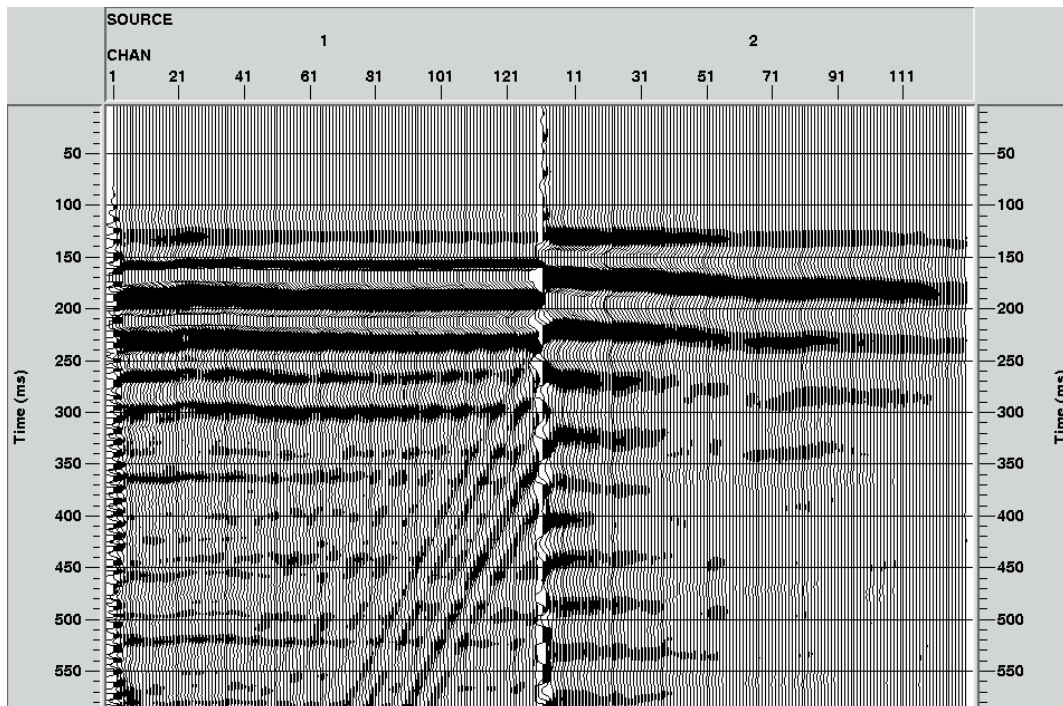


FIG. 3. Downgoing P wavefield from P-source (left) and downgoing S wavefield from S-source (right) displayed using single scalar.

Compared to the P-wave data (Figure 3), the S-wave amplitude decays faster than the P-wave, and has less high-frequency components. It is clearer in Figure 4, when we plot three single traces of station #3, #66 and #129. The P-wave has little phase change. Meanwhile, the S-wave shows a considerable phase change along the same ray-path and same distance.

It makes sense: S-wave travels slower than P-waves. At the near surface, V_P/V_S could be 4-6. Therefore, the S-wavelength is 4-6 times shorter than P-wave. To travel the same distance in a media with even $Q_P=Q_S$, energy will attenuate much more for S-waves, especially for high-frequency components. So, attenuation has bigger impact on S-waves, and more importantly, on the phase of S-waves.

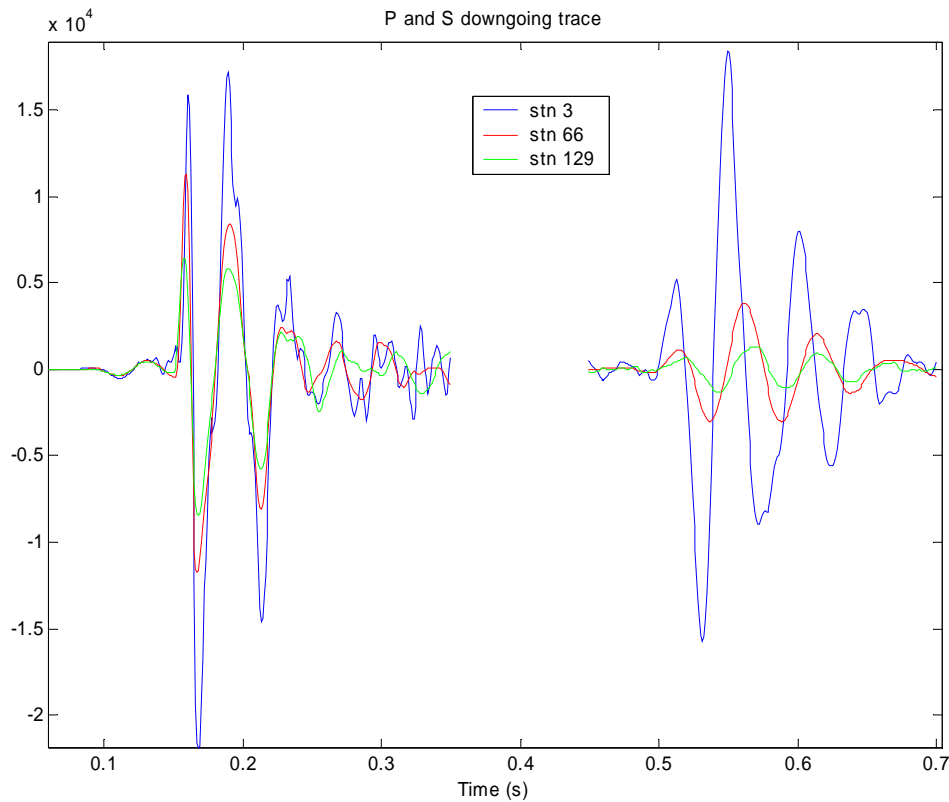


FIG. 4. Traces of P-down and S-down at station #3 (214m depth, blue line), station #66 (685m depth, red line) and station #129 (1157.5m depth, green line).

Q_P ESTIMATION

The spectral ratio method is often used in estimating Q (Xu, et al., 2001). Here, we use a different approach: by setting the surface as the reference level which is constant, we calculate the spectral ratio between any trace and the surface sweep, instead of calculating the spectra ratio between any two traces, which means we obtain Q_{ave} instead of Q_{int} . The energy generated at the surface by the vibrator is designed to have a largely flat spectrum across a given band. Figure 5 displays the spectra of surface sweep, a shallow station (220m) and a deep station (1157m) for both P-wave and S-wave.

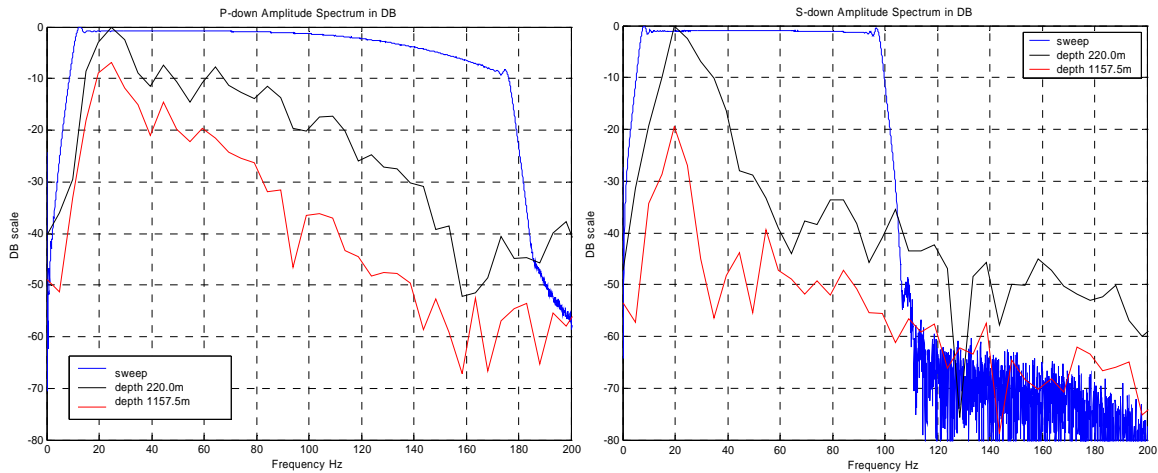


FIG. 5. The amplitude spectrum of the sweep (blue line), station #4 (220m depth, black line) and station #129 (1157.5m depth, red line), for P-source (left) and S-source (right).

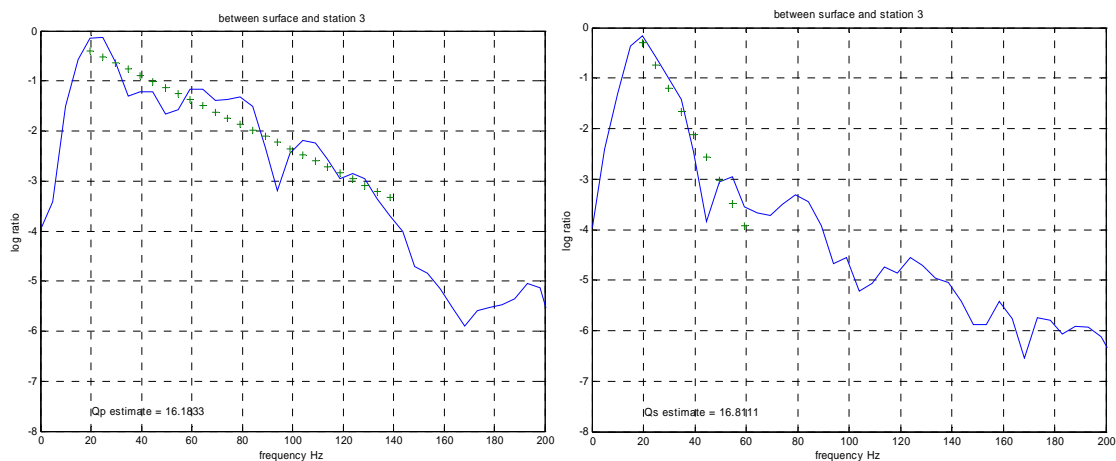


FIG. 6. Using spectra ratios to estimate the Q between surface and station #3 of 214m depth: $Q_{P_ave}=16$ (left) and $Q_{S_ave}=16$ (right).

By using the spectra ratio method, the average Q_p and Q_s between the surface to every geophone depth level are calculated. Figure 6 shows one example of line fitting for the spectra of station #3.

In this way, Q_{p_ave} and Q_{s_ave} curves for the whole interval in the well are calculated and plotted against depth (Figure 7). We note that Q_{p_ave} and Q_{s_ave} have different trends.

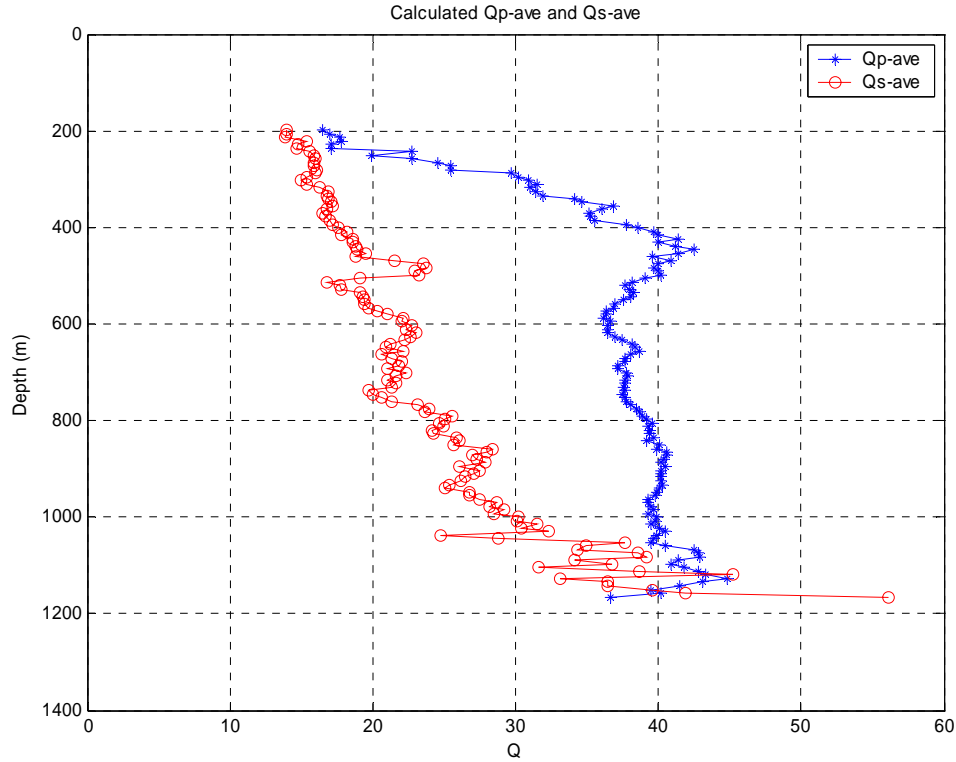


FIG. 7. Average Q_P (blue) and average Q_S (red) curve.

To calculate Q_{int} in a layered model (Bale, et al., 2002), we use:

$$\frac{T(n+1)}{Q_{ave}(n+1)} = \frac{T(n)}{Q_{ave}(n)} + \frac{T(n+1) - T(n)}{Q_{int}(n+1)}, n=1, 2, \dots, N-1 \quad (3)$$

where we have the convention of $Q_{int}(1) = Q_{ave}(1)$.

From equation (3), Q_{int} depends on the relationship between $\frac{T(n)}{Q_{ave}(n)}$ and $\frac{T(n+1)}{Q_{ave}(n+1)}$:
to have $Q_{int} > 0$, we must have:

$$\frac{T(n+1)}{Q_{ave}(n+1)} > \frac{T(n)}{Q_{ave}(n)} \quad (4)$$

If $\frac{T(n+1)}{Q_{ave}(n+1)} - \frac{T(n)}{Q_{ave}(n)}$ is very small, the Q_{int} calculation is unstable.

So, the ratio of first break time and estimated average Q factor, $\frac{T(n)}{Q_{ave}(n)}$, is acting as a quality indicator for Q estimation (denoted as QQI). Figure 8 shows the QQI curves for P- and S-wave.

Fortunately, we have a very well-behaved Q_{I_P} curve from about 400m to 1050m – steadily increase or a slowing-changing positive slope. When we see the curve has a negative slope – decrease – i.e. 200m to 400m for Q_{I_P} (blue line), the derived Q_{p_int} from any two points in this interval will be a negative value. A nearly vertical line (the kinks at 600m and 800m) would result in a very high Q_{p_int} . Smoothing can improve Q_{int} by sweeping out small kinks, but can't change the trend, which means we cannot get a Q_p shallower than 400m in this case.

However, the curve Q_{I_S} is not as good as Q_{I_P} .

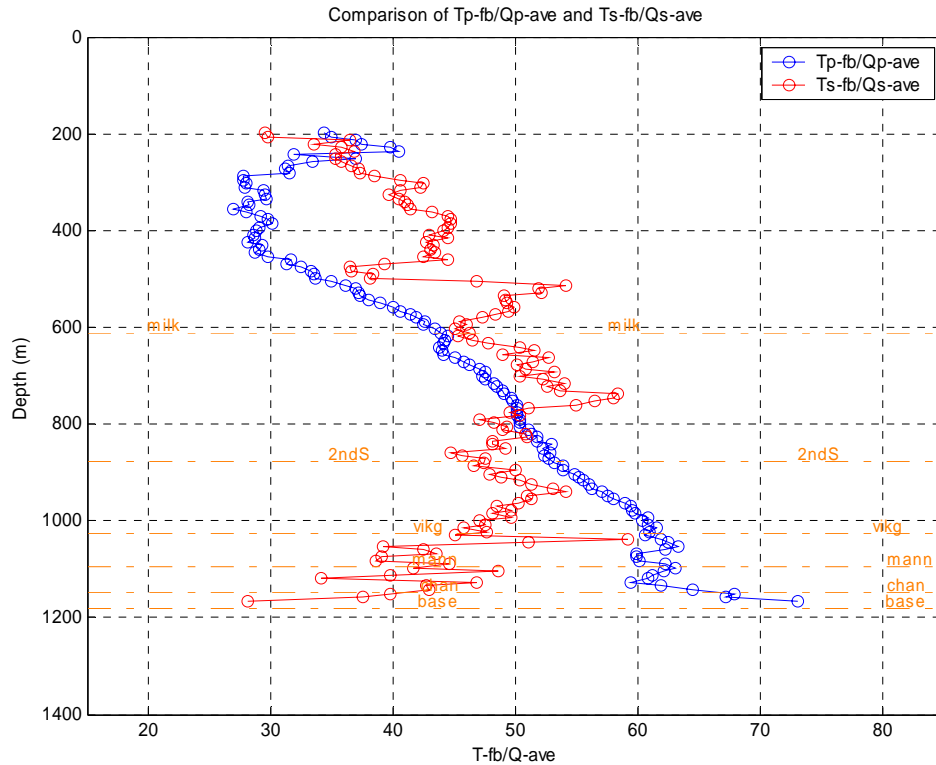


FIG. 8. Q Quality Indicator (QQI) for Q_p (blue) and Q_s (red), with formation tops.

Now we know that we can have a fairly reasonable interval Q_p estimation for a depth range of 450m to 1050m. Getting Q_{ave} first also leaves us room for smoothing. To avoid a jumping Q_{int} , different sizes of boxcar smoothing operators are tried to smooth Q_{ave} . Then, Q_{int} is calculated by equation (3), which is plotted in Figure 9. It is shown that with 10 and 20 samples smoothing, Q_{int10} (black line) and Q_{int20} (red line) still have high positive value spikes at about 800 m depth. The curve of Q_{int30} (blue line), which has 30 samples smoother on Q_{ave} , shows a good shape and is the final version of our estimation.

As mentioned above, the Q_{I_S} curve (Figure 8) doesn't demonstrate a tidy trend as good as Q_{I_P} curve does: a steady increase. Therefore, we didn't try to calculate Q_{s_int} . A future study will be focused on the investigation of reliable Q_s estimation.

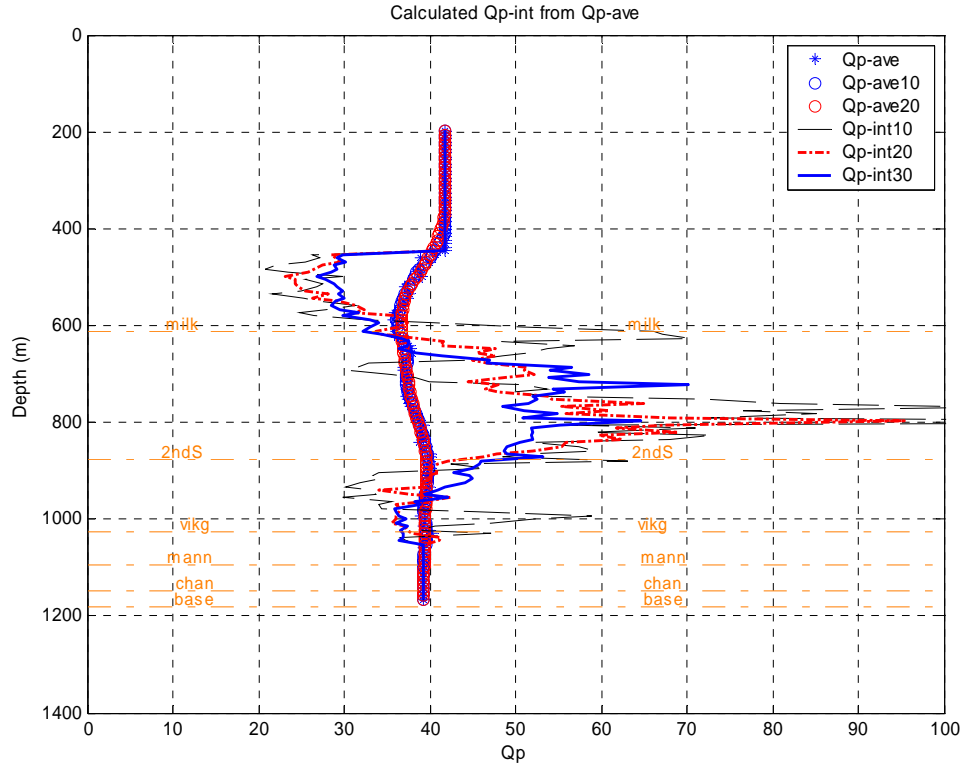


FIG. 9. Average Q_p with 10, 20 and 30 samples smoothing, and derived interval Q_p .

Q_P AND V_P/V_S

Rock physics provides a theoretical relationship, derived from complex elastic moduli, relating the P-wave, S-wave, and bulk compressional Q values, Q_P , Q_S , and Q_K , as follows (e.g. Winkler and Nur, 1979):

$$\frac{1}{Q_P} = \frac{4}{3} \left(\frac{V_S}{V_P} \right)^2 \frac{1}{Q_S} + \left[1 - \frac{4}{3} \left(\frac{V_S}{V_P} \right)^2 \right] \frac{1}{Q_K} \quad (5)$$

Assuming an infinite value for Q_K , Udias (1999) gives:

$$\frac{1}{Q_P} = \frac{4}{3} \left(\frac{V_S}{V_P} \right)^2 \frac{1}{Q_S} \quad (6)$$

Since Q_S estimation is unlikely reliable here, we only investigate the relationship between Q_P and $(V_S/V_P)^2$. We use the first arrival P-wave time (T_P), the first arrival S-wave time (T_S), and the depth of each downhole geophone to calculate the interval V_P/V_S curve. Both T_P and T_S are smoothed by a 10-sample boxcar to get a smoothed V_P/V_S_{int10} .

In order to compare with Q_{P_int30} , both $(V_S/V_P)^2$ from the VSP data and V_P from the sonic log are scaled properly and plotted in the same figure with Q_P , Figure 10. We see all three curves are following the same trend and tracking each other. Although there is no Q_S , the Q_P shows a reasonable correlation with $(V_S/V_P)^2$.

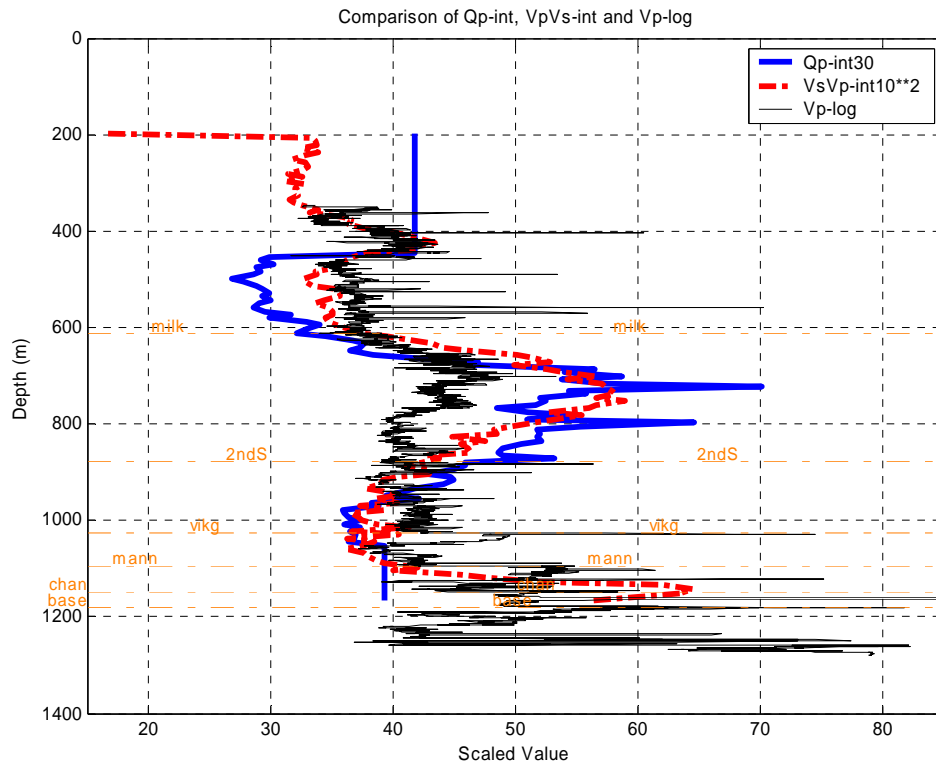


FIG. 10. Smoothed interval Q_P (blue), VSP derived $(V_S/V_P)^2$ (red, scaled) and V_P from sonic log (black, scaled). Both $(V_S/V_P)^2$ and V_P _log are scaled into Q range for comparison.

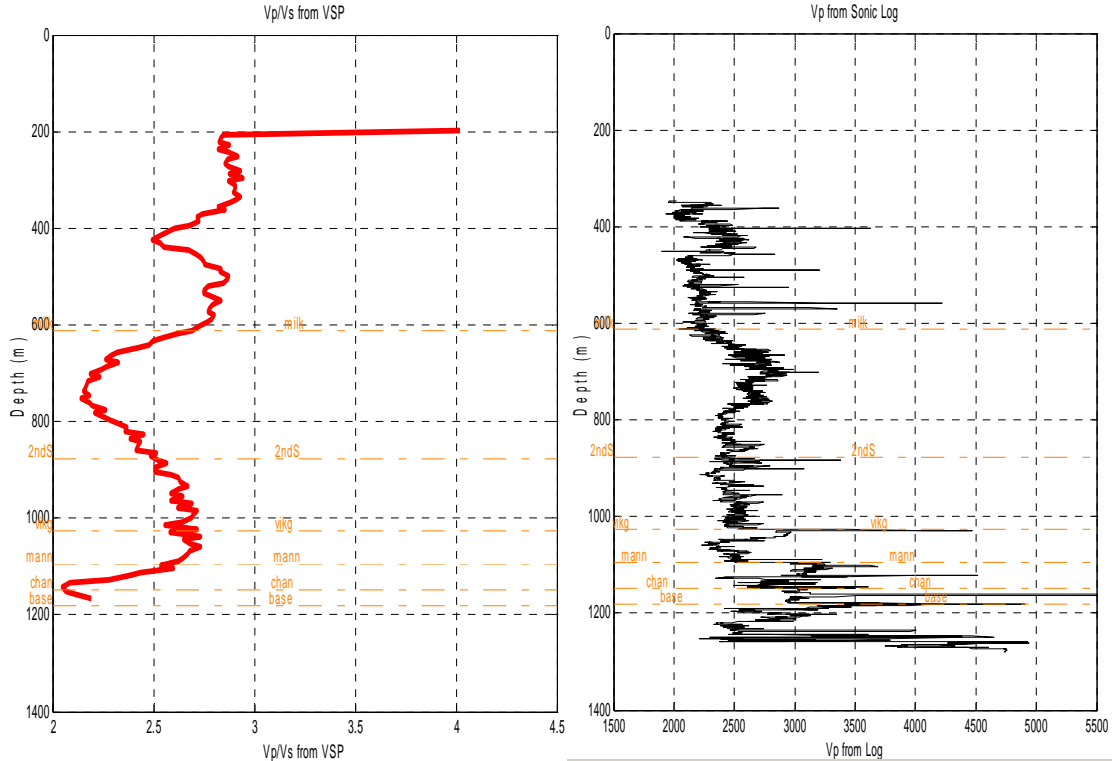


FIG. 11. Smoothed V_P/V_S from VSP (left, red) and V_P from sonic log (right, black).

Thus, we believe our derived $Q_{P_int}30$, the continuous interval Q_P curve from 440 m to 1050 m in this well, is a reliable Q_P estimation. Certainly further smoothing can be applied.

From Figures 10 and 11, the following table has been obtained.

Table 1: Q_P , V_P/V_S and V_P for main geological formations in Ross Lake.

	Q_P	V_P/V_S	V_P (m/s)
400m - 610m (above Milk River)	~ 30	2.8	~ 2200
610m - 870m (Milk River ~ K2WS)	~ 55	2.3	~ 2700
870m - 1050m (K2WS – Mannvile)	~ 40	2.7	~ 2500

DISCUSSION

In Figure 8, the QQI_P curve shows a negative slope from 200m to 400m, which means that the amplitudes of high frequency components are increasing with depth. This is not physical. A possible reason for this is the coupling between the casing and formation: The quality of the cement bond might be bad at this interval. Be noticed that for first break picking, corridor stack, or VSP-CDP mapping, poor cementing won't be a severe problem. In this case, the FIRST trustable Q_{ave} is about 40 at about 445m depth. So, the shallower part $Q_{ave} \sim 18$ at about 200m may not be reliable.

As the VSP is acquired from the bottom of the well up, the source may be changing its frequency content as it continues to shake. To some extents, this disagrees with the assumption of a constant source. We should use a monitor geophone than the vibrator sweep. However, relatively speaking, we suppose the magnitude of the changes between sources are much less than the magnitude of the changes between geophones.

Q_S is difficult to estimate using this method. Looking at Figure 8, we can sparsely pick a few points between 200m to 750m and get a few chunked Q_S . Below 750m, it's hard to follow a positive slope. The reason is possibly on this method itself. S-wave attenuates faster, which results in a much narrower frequency band width at same depth compared with P-wave, for instance, 10-50 Hz versus 10-140 Hz for this data. So the error increases when draw a line to fit the shape of spectra ratio.

Picking different first break times, i.e., systematically pick 2nd peak rather than the first peak, will change the slope of Q_{ave} . But QQI curves are exact same.

CONCLUSION

Using the spectral ratio concept, a new approach to calculate Q has been developed. A reliable continuous interval Q_P curve from about 450m to 1050m in well 11-25 of Husky's Ross Lake oilfield has been derived from a zero-offset VSP by this approach. Meanwhile, a quality indicator for Q estimation (QQI) using spectra ratio method has been established. This QQI curve reveals why sometimes the normal spectra ratio method

gives jumping results, negative Q and unstable Q . Directly from the QQI curve, we can know where there will be a reliable Q estimation. A continuous Q_S is unlikely to be derived using this approach in this case. A future study will focus on the investigation of reliable Q_S estimation.

The VSP-derived Q_P curve has a good correlation with the VSP-derived $(V_S/V_P)^2$ curve and with a V_P curve from well log data as well. Finally, the bulk value of Q_P , V_P/V_S and V_P are estimated for three main geological formations.

ACKNOWLEDGEMENTS

The authors would like to thank Husky Energy Inc. for providing the VSP data and well logs in this study.

REFERENCES

- Bale, R.A. and Stewart, R.R., 2002, The impact of attenuation on the resolution of multicomponent seismic data: CREWES Research Report, **14**.
- Tonn, R., 1991, The determination of seismic quality factor Q from VSP data: A comparison of different computational methods: *Geophys. Prosp.*, **39**, 1-27.
- Udias, 1999, A., 1999, *Principles of Seismology*: Cambridge University Press.
- Winkler, K. and Nur, A., 1979, Pore fluids and seismic attenuation in rocks, in Toksöz, M.N. and Johnston, D.H., Ed., *Seismic wave attenuation*: *Soc. of Expl. Geophys.*, 119-122. (Reprinted from *Geophysical Research Letters*, **6**, 1-4).
- Xu, C. and Stewart R.R., 2001, Walkaway VSP Processing and Q estimation: Pikes Peak, Sask., CSEG Annual Conference, 2001.